

Corrosion Inhibition of Copper and α -Brass in 1 M HNO₃ Solution using New arylpyrimido [5, 4-c] quinoline-2,4-dione derivative

A.S.Fouda^{1,*}, M.A.Ismael¹, R. M. Abo Shahba², L.A.Kamel², A.A.El-Naggar¹

¹ Department of Chemistry, Faculty of Science, El-Mansoura University, El-Mansoura- 35516, EGYPT: Fax: +2 050 2202271,

² Department of Chemistry, Faculty of Science (girls branch), El-Azhar University, Cairo, EGYPT

*E-mail: asfouda@hotmail.com

Received: 11 January 2017 / Accepted: 22 February 2017 / Published: 12 March 2017

The efficiency of 5-(3,4-dimethoxyphenyl)-8,10-dimethoxy-1,3-dimethylpyrimido-[5,4-c]quinoline-2,4-dione(PQD) as corrosion inhibitor for Cu and α -brass in 1 M HNO₃ has been tested by weight loss (WL) and electrochemical techniques such as potentiodynamic polarization (PP), electrochemical impedance spectroscopy (EIS) and electrochemical frequency modulation (EFM) techniques. The calculated adsorption thermodynamic parameters indicated that the adsorption was a spontaneous, exothermic process accompanied by a decrease in entropy. The protection efficiency (PE) increases with increasing the dose of the tested organic compound in HNO₃ solution and decreases with increasing the temperature. The adsorption of the PQD on the Cu and α -brass surfaces in the acid solution was found to obey Langmuir's adsorption isotherm. Scanning electron microscope (SEM) results showed the formation of a protective film on the Cu and α -brass surfaces in the presence of PQD. The results obtained from different techniques were in good agreement

Keywords: Copper, α -Brass, Corrosion inhibition, PQD, HNO₃, EIS, EFM, SEM-EDX

1. INTRODUCTION

Copper is a metal that has a wide range of applications due to its good properties. It is used in electronics, for production of wires, sheets, tubes, and also to form alloys [1-3].Cu is easily combined with many metals. It forms with zinc brasses, which have a higher corrosion resistance and a very easy manufacture. Moreover, brasses are harder and solid. However, their exhibition in acid media creates problems of corrosion [4-8]. When the brasses, containing more than 15% of zinc, are exposed in corrosive environments, they are affected not only by general corrosion damage, but also by

dezincification process involving preferential dissolution of zinc, leaving a spongy mass of Cu on the alloy surface [9].

The use of Cu corrosion inhibitors in acid solutions is usually to minimize the corrosion of Cu during the acid cleaning and descaling. The possibility of the Cu corrosion prevention has attracted many researchers so until now numerous possible inhibitors have been investigated [10-12]. The inhibiting action of these inhibitors is attributed to their adsorption to the metal/solution interface. It has been observed that adsorption depends mainly on certain physico-chemical properties of the inhibitor structural features; Like functional groups, aromaticity, electron density at the donor atoms and π -orbital character of donating electrons. It is noticed that presence of heteroatoms such as nitrogen, sulphur, phosphorous in the organic compound molecule improves its action as corrosion inhibitor. Amongst them there are greater number of organic compounds and their derivatives such as azoles [13-20], amines [21-27], amino acids [28, 29] and many others. It is assumed that the inhibitor should have active centers of adsorption [30]. The toxicity of most corrosion inhibitors made us heading for the use of environment-friendly inhibitors [31].

The objective of this article is to study the action of PQD as non-toxic corrosion inhibitor for Cu and α -brass in 1M HNO₃ solution using different techniques. The surface analysis of Cu and α -brass were studied by SEM and energy dispersive X-ray (EDX) techniques.

2. EXPERIMENTAL

2.1 Materials

The experiments were performed with local commercial Cu and α -brass (Helwan Company of Non-Ferrous Industries, Egypt) with the following composition (weight %)

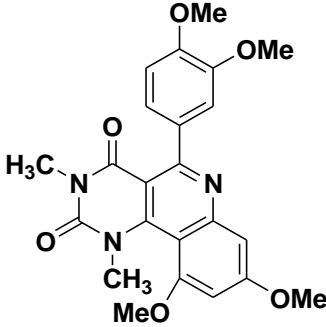
Element	Zn	Ca	S	Si	Cu
Weight %	0.155	0.73	0.031	0.21	98.80

Element	Pb	Fe	Zn	Cu
Weight %	2.17	0.061	39.58	58.07

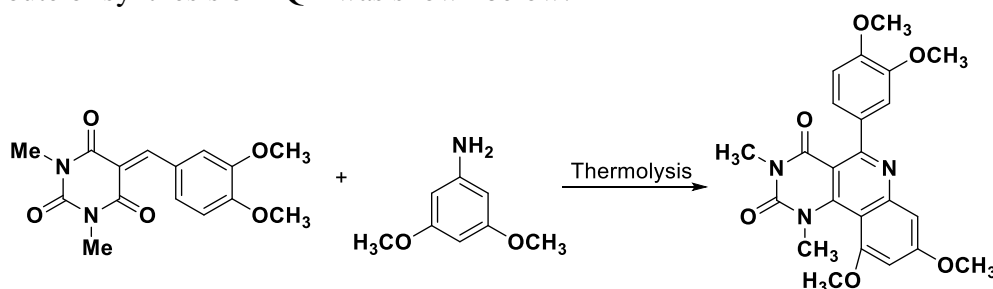
2.2 Chemicals

The aggressive acid solutions were prepared by dilution of analytical grade (67.5%) HNO₃ with twice distilled water. The entire chemical used was obtained from Aldrich chemical company. The dose range of the PQD used was 1×10^{-6} - 20×10^{-6} M. The PQD was prepared as recently reported [34].

The structure, name, molecular weight and molecular formula of PQD are shown below:

Structure/IUPAC name	Chemical formula/ molecular weight
 <p style="text-align: center;">MA-0980</p> <p>IUPAC name: 5-(3,4-Dimethoxyphenyl)-8,10-dimethoxy-1,3-dimethylpyrimido[5,4-c]quinoline-2,4-dione (PQD)</p>	$C_{23}H_{23}N_3O_6$ (437.45)

The route of synthesis of PQD was shown below:



Scheme 1. Synthesis of pyrimido [5,4-c]quinoline-2,4-dione derivative MA-0980.

2.3. Weight loss (WL) measurements

The samples used were machined to be a rectangular (2 x 2 x 0.3 cm). Polishing of the samples was done mechanically with speed polisher. The samples were polished with emery paper up to grade 1200 grit size. After being polished they were rinsed in acetone, dried, and wrapped in filter paper. The samples were rinsed in twice distilled water and wiped dry before dipping them in the test solution. After that, the specimens were dipped in 100 ml of 1 M HNO₃ with and without different doses of PQD at different temperatures. After different immersion periods (30, 60, 90, 120, 150 and 180 min) the Cu coupons were taken out, washed with twice distilled water then dried and weighted accurately. The inhibition efficiency (PE %) and surface coverage (Θ) were calculated from:

$$PE \% = \theta \times 100 = [1 - (W / W^{\circ})] \times 100 \quad (1)$$

Where W° and W are the weight losses in the nonexistence and existence of inhibitor, respectively.

2.3. Electrochemical measurements

All the electrochemical measurements were performed using the electrochemical workstation (Gamry PCI4-G750 Instruments) and a constant temperature of 25°C is maintained in the acid

medium. Prior to the electrochemical measurements, all samples were prepared according to the procedure described above. The platinum electrode and saturated calomel electrode (SCE) were used as auxiliary and reference electrodes, respectively. The working electrodes constitute Cu or α -brass specimens of one cm² area. The tip of the reference electrode is positioned very close proximity to the working electrode surface by the use of fine Luggin capillary in order to minimize ohmic potential drop. Remaining uncompensated resistance was also reduced by electrochemical workstation. Each experiment was repeated at least three times to check the reproducibility.

PP studies were carried out at a scan rate of 1 mV s⁻¹. The electrode potential was allowed to stabilize for 35 min until a constant potential was reached, which is referred as the OCP. In all the cases, OCP was established first, and then the polarization experiment was carried out. The polarization curves for Cu specimens in the test solution with and without various doses of PQD were recorded from -1000 to 1000 mV at open circuit potential. Then icorr was used for the calculation of PE and surface coverage (θ) as below [35]:

$$\% \text{ PE} = \theta \times 100 = [1 - (i_{\text{corr}}/i_{\text{corr}}^{\circ})] \times 100 \quad (2)$$

The EIS studies were carried out in the same setup used for PP studies described above. We applied the ac perturbation signal of 10 mV within the frequency range of 100 kHz to 0.2 Hz. All electrochemical impedance measurements were carried out at open circuit potential. The PE and the surface coverage (θ) obtained from the impedance measurements are defined by the following relation:

$$\text{PE}\% = \theta \times 100 = \left[1 - \left(\frac{R_{\text{ct}}^{\circ}}{R_{\text{ct}}} \right) \right] \times 100 \quad (3)$$

Where R^oct and Rct are the charge transfer resistances in the nonexistence and existence of PQD, respectively.

EFM tests were carried out using two frequencies of 2 and 5 Hz. The base frequency was 0.1 Hz, so that the wave form repeats after 1 s. The intermodulation spectra contain current responses assigned for harmonical and intermodulation current peaks. The larger peaks were used to calculate the corrosion current density (i_{corr}), the Tafel slopes (β_c and β_a) and the causality factors CF-2 & CF-3 [36].

2.4. Surface analysis

The surface films were formed on the Cu specimens by dipping them in inhibitor solution for a period of 24 h. After the immersion period, the specimens were taken out, dried and the nature of the film formed on the surface of the metal specimen was analyzed by EDX and SEM techniques. Analysis was carried out by Hitachi S-550 Scanning Electron Microscope. Rough elemental analyses for the exposed surface were conducted by EDX technique.

3. RESULTS AND DISCUSSION

3.1. WL measurements

WL measurements for Cu and α -brass were carried out in 1 M HNO₃ in the nonexistence and existence of different doses of PQD is shown in Figs (1&2). Corrosion rates (CR) of Cu and α -brass in

($\text{mg cm}^{-2} \text{ min}^{-1}$) and the PE% were calculated and recorded in Table 1. The results showed that PQD inhibit the corrosion Cu and α -brass in 1 M HNO_3 solutions.

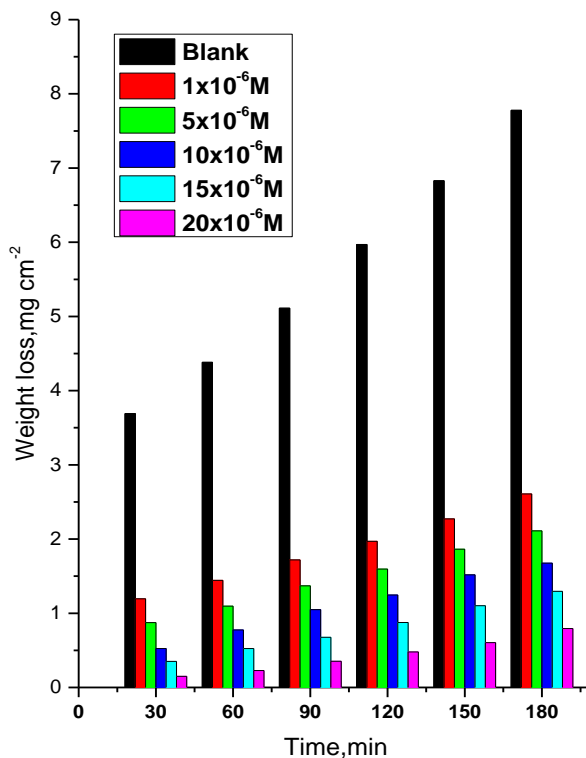


Figure 1. WL-time curves for the corrosion of Cu in 1 M HNO_3 in the nonexistence and existence of different doses of PQD at 25°C

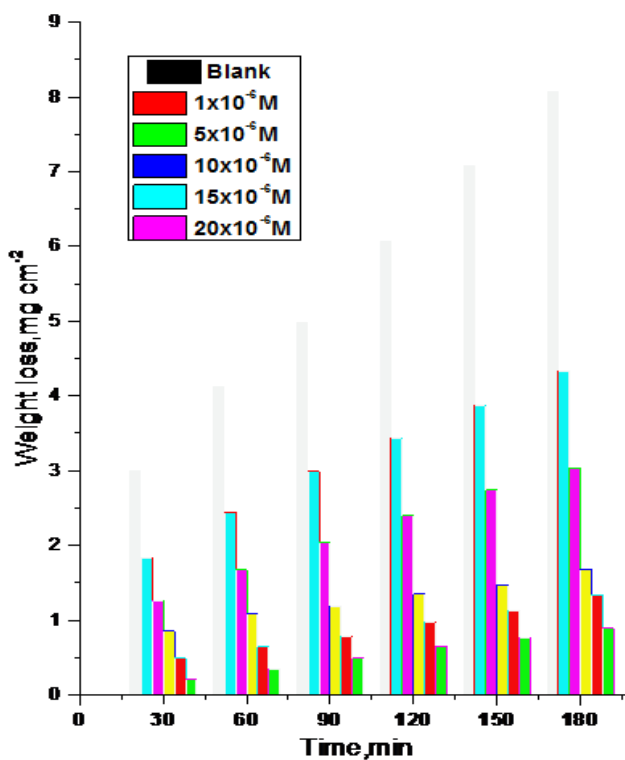


Figure 2. WL-time curves for the corrosion of α -brass in 1 M HNO_3 in the nonexistence and existence of different doses of PQD at 25°C.

The CR was found to depend on the dose of the PQD. Increasing the dose of each PQD increases the PE% which reached its maximum value at dose 20×10^{-6} M for the Cu and α -brass. This indicates that the protective effect of PQD is not solely due to their reactivity with the nitric acid. The inhibitory behavior of PQD against Cu and α -brass corrosion can be attributed to the adsorption of it on the Cu and α -brass surface, which limits the dissolution of the latter by blocking of their corrosion sites and hence decreasing the CR, with increasing efficiency as their doses increase [37].

Table 1. CR in and PE data obtained from WL measurements for Cu and α -brass in 1 M HNO₃ solutions without and with various doses of PQD at 25°C

Compound	Conc, M	Wt loss, mgcm ⁻²	C.R., (mgcm ⁻² min ⁻¹)	θ	% IE
Blank	0.0	5.970	0.050	----	----
Cu	1×10^{-6}	1.970	0.016	0.670	67.0
	5×10^{-6}	1.596	0.013	0.733	73.1
	10×10^{-6}	1.246	0.010	0.791	79.3
	15×10^{-6}	0.876	0.007	0.863	86.3
	20×10^{-6}	0.479	0.004	0.912	91.5
Blank	0.0	6.08	0.051	----	----
α -brass	1×10^{-6}	3.43	0.039	0.435	43.5
	5×10^{-6}	2.39	0.020	0.605	60.5
	10×10^{-6}	1.34	0.011	0.779	77.9
	15×10^{-6}	0.97	0.008	0.839	83.9
	20×10^{-6}	0.64	0.005	0.894	89.4

3.1.1. Effect of temperature and activation parameters of corrosion process

The effect of temperature, in the range of 25–40°C with an increment of 5°C on both the CR and the PE of different doses of PQD was studied by WL tests and was given in Tables (2&3).

Table 2. Data of WL tests for Cu in 1 M HNO₃ solution in the nonexistence and existence of different doses of PQD at 25–40°C

Conc., ppm	Temp., °C	C.R., (mgcm ⁻² min ⁻¹)	θ	%IE
1×10^{-6}	25	0.016	0.670	67.0
	30	0.018	0.662	66.2
	35	0.024	0.586	58.6
	40	0.027	0.560	56.0

5 x 10⁻⁶	25	0.013	0.733	73.2
	30	0.015	0.717	71.7
	35	0.019	0.681	68.1
	40	0.021	0.664	66.4
10 x 10⁻⁶	25	0.010	0.791	79.1
	30	0.011	0.787	78.7
	35	0.014	0.756	75.6
	40	0.017	0.728	72.8
15 x 10⁻⁶	25	0.007	0.863	86.3
	30	0.008	0.854	85.4
	35	0.011	0.819	81.9
	40	0.013	0.791	79.1
20 x 10⁻⁶	25	0.004	0.912	91.1
	30	0.005	0.908	90.8
	35	0.008	0.861	86.1
	40	0.009	0.851	85.1

Table 3. Data of WL tests for α -brass in 1 M HNO₃ solution in the nonexistence and existence of different doses of PQD at 25–40°C

Conc., M	Temp., °C	CR, (mgcm ⁻² min ⁻¹)	Θ	% PE
1 x 10⁻⁶	25	0.033	0.435	43.5
	30	0.036	0.379	37.9
	35	0.038	0.353	35.3
	40	0.043	0.293	29.3
5x 10⁻⁶	25	0.023	0.605	60.5
	30	0.025	0.569	56.9
	35	0.026	0.554	55.4
	40	0.037	0.400	40.0
10 x 10⁻⁶	25	0.011	0.779	77.9
	30	0.015	0.735	73.5
	35	0.016	0.725	72.5
	40	0.024	0.610	61.0
15 x 10⁻⁶	25	0.008	0.839	83.9
	30	0.010	0.823	82.3
	35	0.011	0.811	81.1
	40	0.020	0.679	67.9
20x 10⁻⁶	25	0.005	0.894	89.4
	30	0.007	0.784	78.4
	35	0.008	0.865	86.5
	40	0.016	0.741	74.1

From Tables (3, 4); we can see that increasing the temperature leads to an increase in the corrosion rate of Cu and α -brass both in free acid and inhibited acid solution and a decrease in the inhibition efficiency of the extract which suggested that corrosion inhibition of Cu by the investigated

compounds caused by the adsorption of inhibitor molecule while higher temperatures caused the desorption of the extract components from the Cu surface [38].

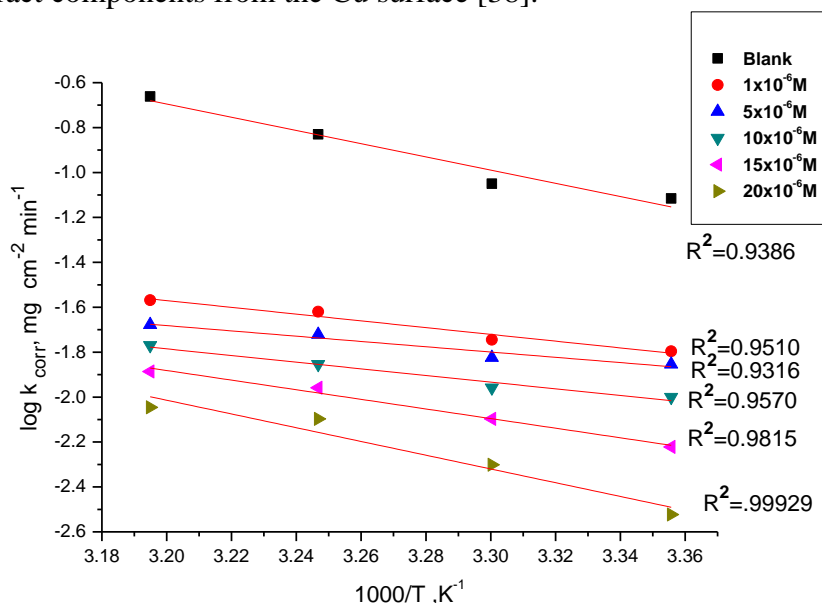


Figure 3. Log k_{corr} -1/T curves for Cu dissolution in 1M HNO_3 in nonexistence and existence of different doses of PQD

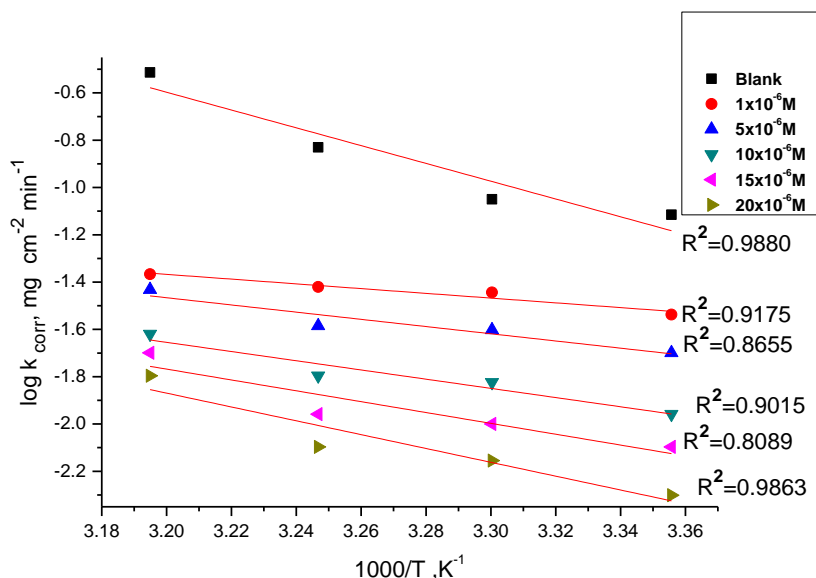


Figure 4. Log k_{corr} -1/T curves for α -brass dissolution in 1 M HNO_3 in nonexistence and existence of different doses of PQD

The apparent activation energy E_a^* , enthalpy of activation ΔH^* , and entropy of activation ΔS^* for the corrosion of samples in 1 M HNO_3 solution in the nonexistence and existence of different doses of PQD at 25-40°C were calculated from Arrhenius-type equation:

$$\log k = \frac{-E_a^*}{2.303 RT} + \log A \tag{4}$$

and transition-state equation:

$$k = \left(\frac{RT}{Nh}\right) \exp\left(\frac{\Delta S^*}{R}\right) \exp\left(\frac{\Delta H^*}{RT}\right) \tag{5}$$

where A is the frequency factor, h is Planck's constant, N is Avogadro's number, and R is the universal gas constant.

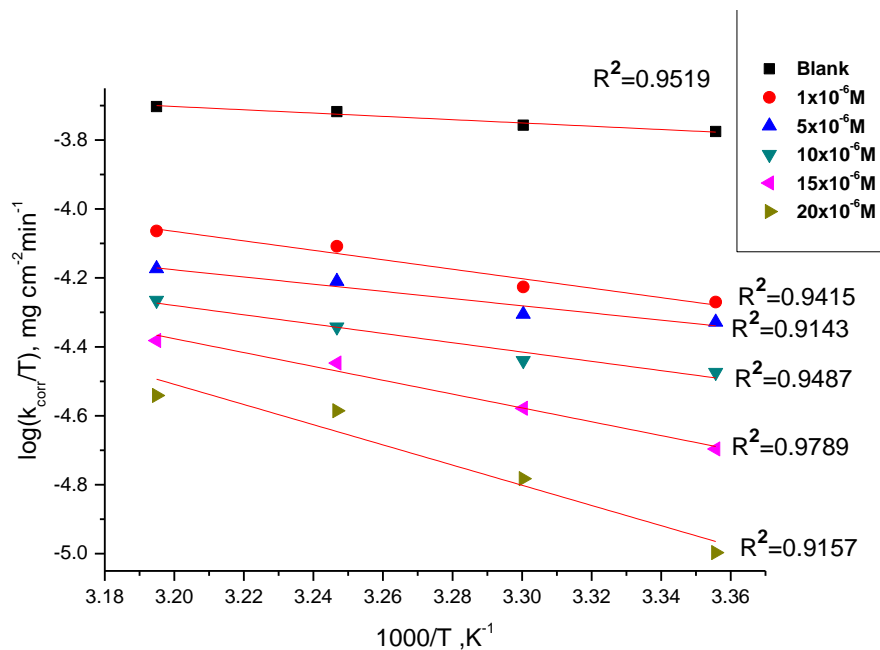


Figure 5. Log $k_{corr}/T-1/T$ curves for Cu dissolution in 1 M HNO₃ in nonexistence and existence of different doses of PQD

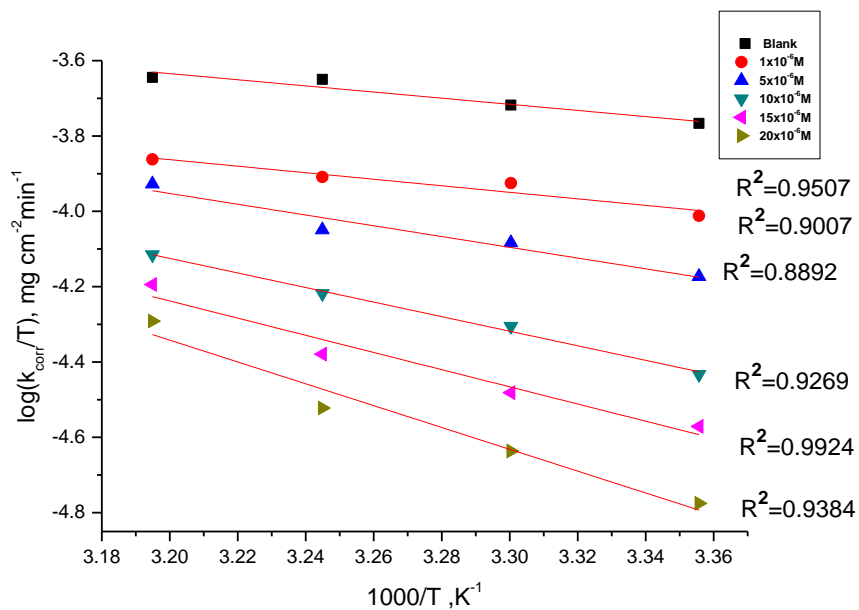


Figure 6. Log $k_{corr}/T-1/T$ curves for α-brass dissolution in 1M HNO₃ in nonexistence and existence of different doses of PQD

A plot of log rate (k) vs. $1/T$ and $\log(k/T)$ vs. $1/T$ give straight lines with slope of $-E_a^*/2.303R$ and $\Delta H^*/2.303R$, respectively. The intercept will be A and $\log(R/Nh) + (\Delta S^*/2.303R)$ for Arrhenius and transition state equations, respectively.

Figures (3, 4) represent plots of $\log k$ vs. $1/T$ and Figures (5, 6) represent plots of $\log(k/T)$ vs. $1/T$ data. The calculated values of the apparent activation energies, E_a^* , activation entropies, ΔS^* , and activation enthalpies, ΔH^* , are given in Table 4. The almost similar values of E_a^* suggest that the inhibitors are similar in the mechanism of action. Also, the values of activation energy E_a^* increase in the same order of increasing inhibition efficiency of the inhibitor. It is also indicated that the whole process is controlled by surface reaction, since the energy of activation corrosion process is over 20 kJ mol^{-1} [39].

From the results of Table 5, it is clear that the presence of PQD increases the activation energy values and consequently decreases the CR of the Cu and α -brass. Also, activation energy increases by increasing the dose of PQD. These results indicate that this tested compound acts as inhibitor through increasing activation energy of Cu dissolution by making a barrier to mass and charge transfer by its adsorption on Cu surface.

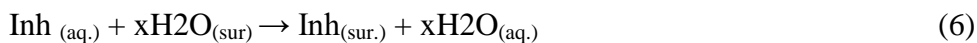
Table 4. Effect of doses of PQD on the activation energy of Cu and α -brass dissolution in 1 M HNO_3

Comp	Conc, $\times 10^6$ M	$-E_a^*$	$-\Delta H^*$	$-\Delta S^*$
		kJ mol^{-1}	kJ mol^{-1}	$\text{J mol}^{-1} \text{K}^{-1}$
Cu	1	22.5	3.9	191.3
	5	28.3	8.6	213.6
	10	28.8	11.2	196.8
	15	40.9	16.6	158.3
	20	58.6	24.3	104.4
α -brass	1	19.2	6.7	217.2
	5	29.1	7.2	218.4
	10	37.2	11.8	185.7
	15	43.9	16.0	158.1
	20	56.0	18.9	139.0

The activation enthalpy (ΔH^*) was found to increase in the presence of the PQD, implies that the addition of the inhibitor to the acid solution increases the height of the energy barrier of the corrosion reaction to an extent depends on the type and dose of the PQD [40]. The entropy of activation (ΔS^*) is large and negative, which implies that the activated complex represents association rather than dissociation step. Accordingly, this indicates that a decrease in disorder takes place, going from reactants to the activated complex [41].

3.1.2. Adsorption isotherms

Organic molecules inhibit the corrosion process by the adsorption on metal surface. Theoretically, the adsorption process can be regarded as a single substitutional process in which an inhibitor molecule (Inh.) in the aqueous phase substitutes an "x" number of water molecules adsorbed on the metal surface [42] vis,



Where x is known as the size ratio and simply equals the number of adsorbed water molecules replaced by a single inhibitor molecule. The adsorption depends on the structure of the inhibitor, the type of the metal and the nature of its surface, the nature of the corrosion medium and its pH value, the temperature, and the electrochemical potential of the metal-solution interface. Also, the adsorption provides information about the interaction among the adsorbed molecules themselves as well as their interaction with the metal surface. Actually an adsorbed molecule may make the surface more difficult or less difficult for another molecule to become attached to a neighboring site and multilayer adsorption may take place. There may be more or less than one inhibitor molecule per surface site. Finally, various surface sites could have varying degrees of activation. A number of mathematical relationships for the adsorption isotherms have been suggested to fit the experiment data of the present work. The θ was calculated from the equation mentioned % PE = (100x θ). The values of θ have been shown in Tables (2&3). The θ was found to increase with increasing dose of the PQD. Attempts were made to fit θ values to various isotherms including Langmuir, Freundlich, Temkin and Frumkin. By far, the best fit was obtained with Langmuir isotherm. The equilibrium constant of the adsorption process, K, which is related to the standard free energy of adsorption ($\Delta G^\circ_{\text{ads}}$) by [43&44]:

$$\frac{C}{\theta} = \frac{1}{K} + C \quad (7)$$

Figures (7&8) show the plot of c / θ vs. C for different doses of PQD. These plots give straight lines with slope very close to unity. The regression (R^2) is more than 0.9. This means that there is no interaction between the adsorbed species on the electrode surface [45]. All the calculated thermodynamic parameters are listed in Table 5. The negative value of $\Delta G^\circ_{\text{ads}}$ in Table 5 suggested that the adsorption of PQD molecules on to Cu and α -brass surface is spontaneous process. Generally, values of $\Delta G^\circ_{\text{ads}}$ up to -20 kJ mol^{-1} are consistent with electrostatic interaction between the charged molecules and the charged metal (physical adsorption) while those more negative than -40 kJ mol^{-1} involve charge sharing or transfer of electrons from the inhibitor molecules to the metal surface to form a coordinate type of bond (chemisorption) [46 & 47]. Moreover, the adsorption heat can be calculated according to the eq. (8) [48]:

$$\Delta G^\circ_{\text{ads}} = \Delta H^\circ_{\text{ads}} - T \Delta S^\circ_{\text{ads}} \quad (8)$$

Figures (9&10) show the plot of ΔG° vs. $1/T$ for Cu and brass dissolution in 1 M HNO₃ in the existence of PQD. The $\Delta H^\circ_{\text{ads}}$ values Table 5 are negative, which show that the adsorption is an exothermic process [49]. Finally, the standard adsorption entropy $\Delta S^\circ_{\text{ads}}$ can be calculated by the equation 9:

$$\Delta S^\circ_{\text{ads}} = \Delta H^\circ_{\text{ads}} - \Delta G^\circ_{\text{ads}}/T \quad (9)$$

$\Delta S^\circ_{\text{ads}}$ values (Table 5) are negative, which show that the adsorption is an exothermic process and always accompanied by a decrease of entropy. The reason can be explained as follows: the

adsorption of organic inhibitor molecules from the aqueous solution. Table 5 lists all the above calculated thermodynamic parameters [50&51].

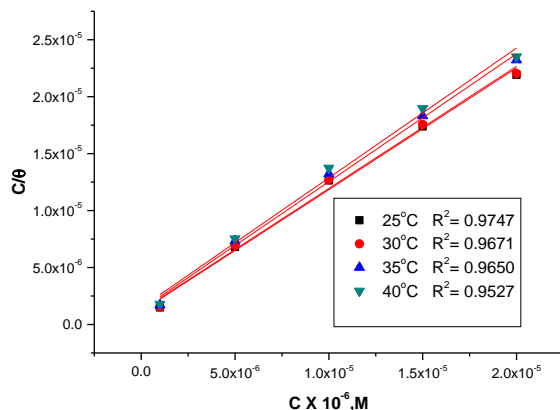


Figure 7. Langmuir adsorption isotherm for PQD on Cu in 1 M HNO3 at different temperatures

Table 5. Thermodynamic parameters for Cu and α-brass in 1 M HNO3 for PQD at 25-40°C

Comp	Temp, K	$K_{ads} \times 10^5 M^{-1}$	$-\Delta G^{\circ}_{ads} kJ mol^{-1}$	$-\Delta H^{\circ}_{ads} kJ mol^{-1}$	$-\Delta S^{\circ}_{ads} J mol^{-1}k^{-1}$
Cu	298	1.41	27.6	12.6	50.9
	303	1.48	28.0		
	308	1.08	28.2		
	313	1.24	28.4		
α-brass	298	4.87	42.2	58.1	135.9
	303	4.55	44.5		
	308	3.49	45.0		
	313	2.33	45.3		

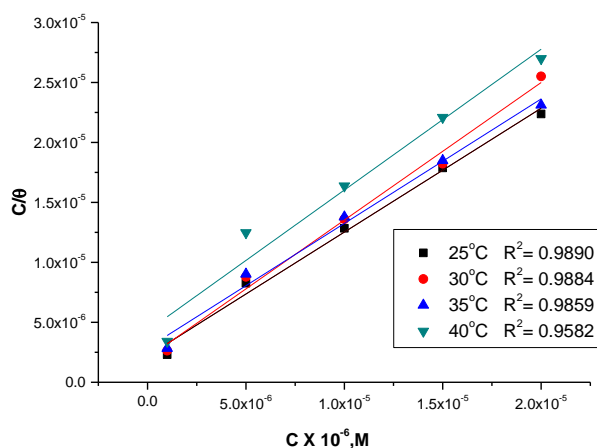


Figure 8. Adsorption isotherm curves for the adsorption of PQD on α-brass in 1 M HNO3 at different temperatures

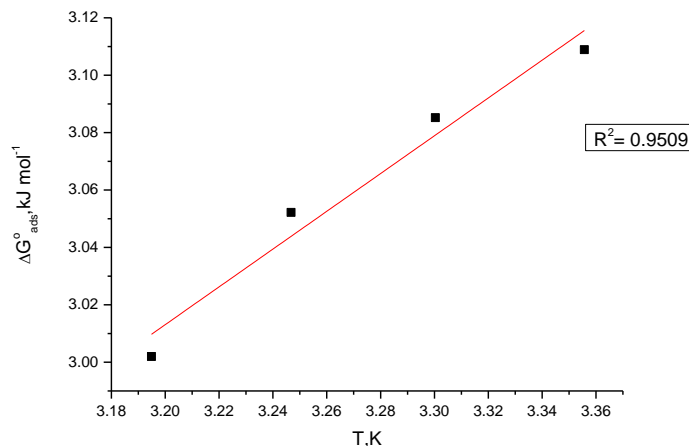


Figure 9. ΔG° vs. $(1/T)$ curves for Cu dissolution in 1 M HNO_3 in the existence of PQD

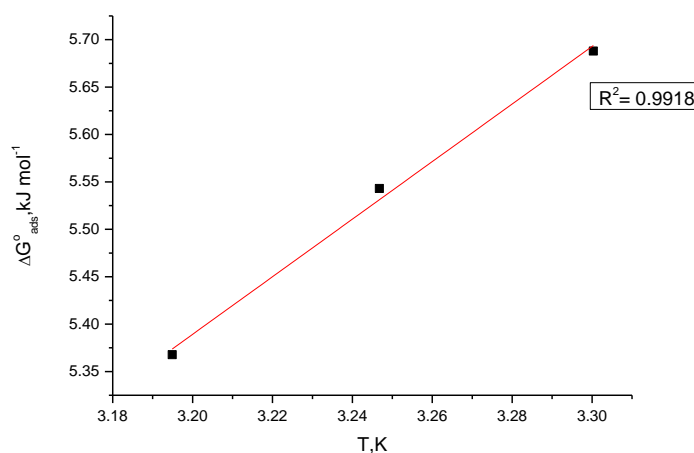


Figure 10. $\Delta G^\circ_{\text{ads}}$ vs. $(1/T)$ curves for Cu dissolution in 1 M HNO_3 in the presence of PQD

3.2. Polarization Curves

Cu can hardly be corroded in the deoxygenated acid solutions, as Cu cannot displace hydrogen from acid solutions according to the theories of chemical thermodynamics [52&53]. PP technique is based on current and potential measurements. It is generally accepted that the inhibitor molecule inhibits corrosion by adsorbing at the metal/solution interface. Figures (11&12) show typical polarization curves for Cu and α -brass in 1 M HNO_3 media. The two distinct regions that appeared were the active dissolution region (apparent Tafel region), and the limiting current region. In the inhibitor-free solution, the anodic polarization curve of Cu showed a monotonic increase of current with potential until the current reached the maximum value. After this maximum current density value, the current density declined rapidly with potential increase, forming an anodic current peak that was related to $\text{Cu}(\text{NO}_3)_2$ film formation. In the presence of PQD both the cathodic and anodic current densities were greatly decreased. Various corrosion parameters such as corrosion potential (E_{corr}), anodic and cathodic Tafel slopes (β_a , β_c), the corrosion current density (i_{corr}), the θ and the % PE are given in Table 6. It can see from the experimental results that in all cases, addition of PQD induced a

significant decrease in cathode and anodic currents. The values of E_{corr} were affected and slightly shifted to more negative direction by the addition of PQD. The lower values of i_{corr} in the presence of PQD without causing significant changes in E_{corr} values and suggest that PQD is mixed type mainly cathodic for Cu and brass.

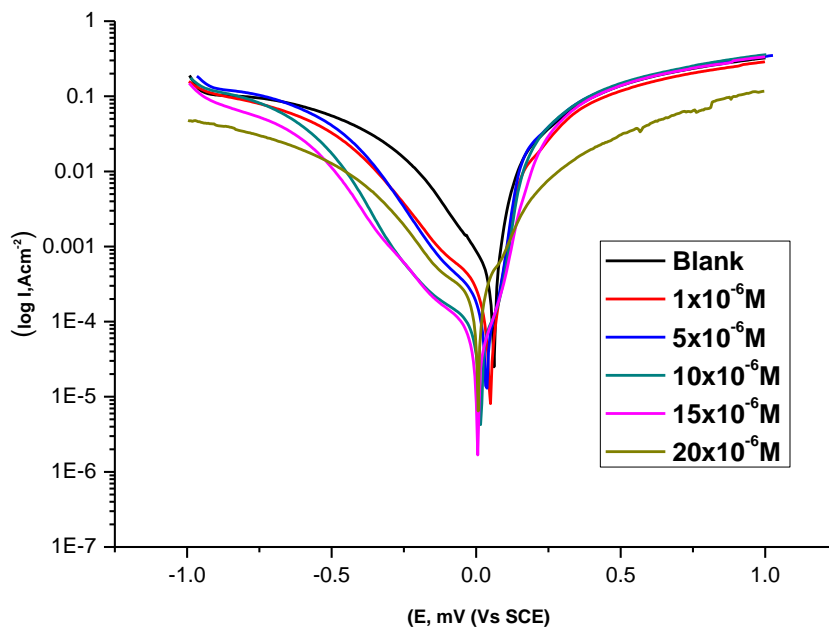


Figure 11. PP curves for the corrosion of Cu in 1 M HNO_3 solution without and with various doses of PQD at 25°C

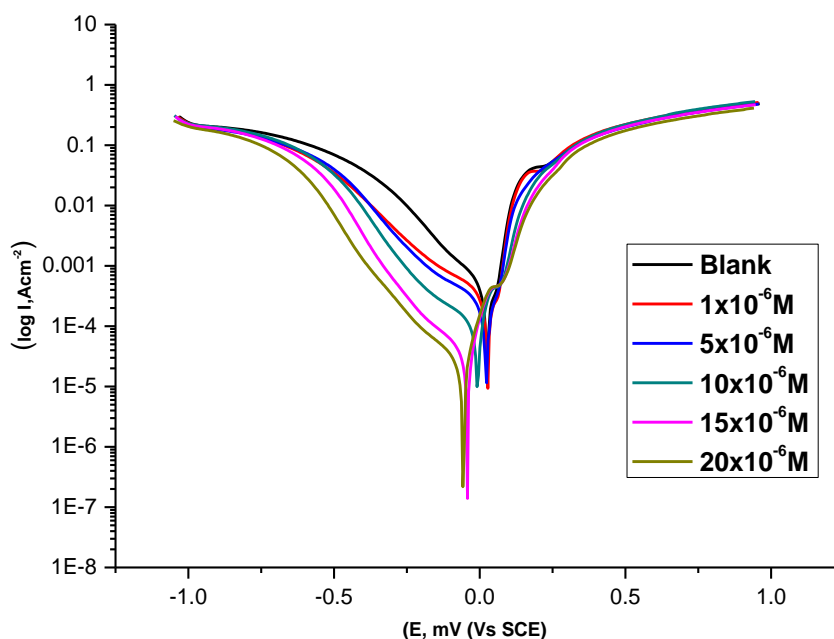


Figure 12. PP curves for the corrosion of α -brass in 1 M HNO_3 solution without and with various doses of PQD at 25°C

Table 6. Effect of dose of PQD on the electrochemical parameters calculated from PP technique for the corrosion of Cu and α -brass in 1M HNO3 at 25°C

Comp.	Conc, $\times 10^6$ M	$-E_{corr.}$, mV(vs SCE)	$i_{corr.}$, $\mu A\ cm^{-2}$	β_a , mV dec $^{-1}$	$-\beta_c$, mV dec $^{-1}$	C.R. mpy	θ	% PE
Cu	Blank	6.06	747	262	644	368	----	----
	1	50.9	169	123	256	83.6	0.773	77.3
	5	14.0	131	103	179	64.6	0.824	82.4
	10	14.1	77.2	116	305	38.0	0.896	89.6
	15	4.69	64.8	124	268	31.9	0.913	91.3
	20	3.80	52.9	110	317	26.1	0.929	92.9
α -Brass	Blank	25.1	462	112	220	227	----	----
	1	60.5	199	48.1	133	156	0.569	56.9
	5	48.5	158	89.5	219	77.9	0.658	65.8
	10	29.7	131	146	238	64.8	0.716	71.6
	15	52.2	128	56	182	62.9	0.722	72.2
	20	53.4	77.3	99.6	143	38.1	0.832	83.2

3.3. EIS tests

EIS is well-established and powerful technique in the study of corrosion. Surface properties, electrode kinetics and mechanistic information can be obtained from impedance diagrams [54-58]. Figures (13&15), Figures (14&16) show the Nyquist and Bode plots obtained at open-circuit potential both in the nonexistence and existence of increasing doses of PQD at room temperature. The increase in the size of the capacitive loop with the addition of PQD shows that a barrier gradually forms on the Cu surface. From the Bode plots the total impedance increases with inhibitor dose (log Z vs. log f). But (log f vs. phase) from Bode plot shows the continuous increase in the phase angle shift, obviously correlating with the increase of inhibitor adsorbed on Cu surface. The Nyquist plots do not yield perfect semicircles as expected from the theory of EIS. The deviation from ideal semicircle was generally attributed to the frequency dispersion [59] as well as to the in homogeneities of the surface.

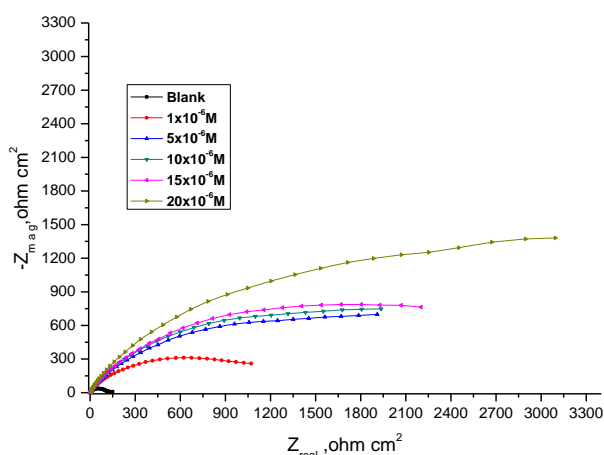


Figure 13. Nyquist plots recorded for Cu in 1 M HNO3 without and with various doses of PQD at 25°C

EIS spectra of the these compounds were analyzed using the equivalent circuit in Figure 17, where R_s represents the solution resistance, R_{ct} denotes the charge-transfer resistance, and a CPE instead of a pure capacitor represents the interfacial capacitance [60]. The impedance of a CPE is described by the following equation:

$$Y_{CPE} = Y_0(j\omega)^n \tag{10}$$

where Y_0 is the magnitude of the CPE, j is an imaginary number, ω is the angular frequency ($\omega_{max} = 2\pi f_{max}$), f_{max} is the frequency at which the imaginary component of the impedance reaches its maximum values, and n is the deviation parameter of the CPE: $-1 \leq n \leq 1$. The values of the interfacial capacitance C_{dl} can be calculated from CPE parameter values Y_0 and n using equation 11[61]:

$$C_{dl} = \frac{1}{2\pi R_{ct} f_{max}} \tag{11}$$

After analyzing the shape of the Nyquist plots, it is concluded that the curves approximated by a single capacitive semicircles, showing that the corrosion process was mainly charged-transfer controlled [62&63]. The general shape of the curves is very similar for all samples (in presence or in absence of inhibitors at different immersion times) indicating that no change in the corrosion mechanism [64]. From the impedance data Table 7, we conclude that the value of R_{ct} increases with increase in dose of the inhibitors and this indicates an increase in % PE.

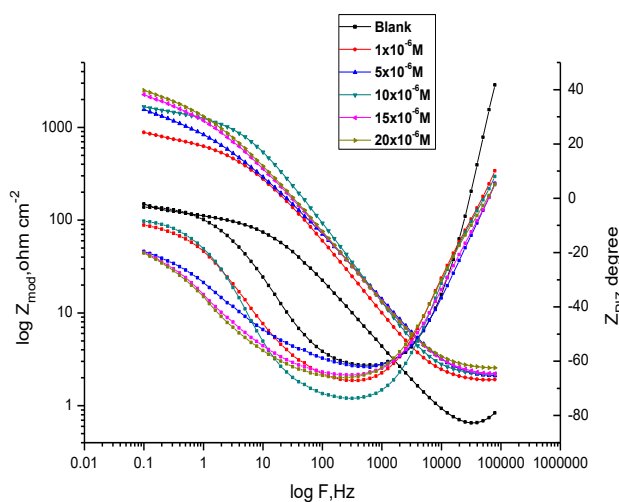


Figure 14. Bode plots recorded for Cu in 1 M HNO₃ without and with various doses of PQD at 25°C

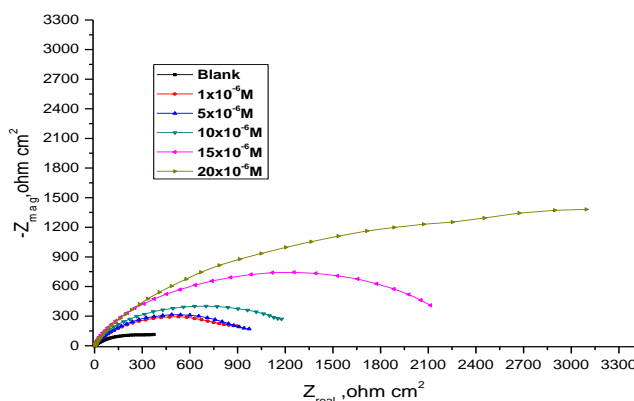


Figure 15. Nyquist plots recorded for brass in 1 M HNO₃ without and with various doses of PQD at 25C

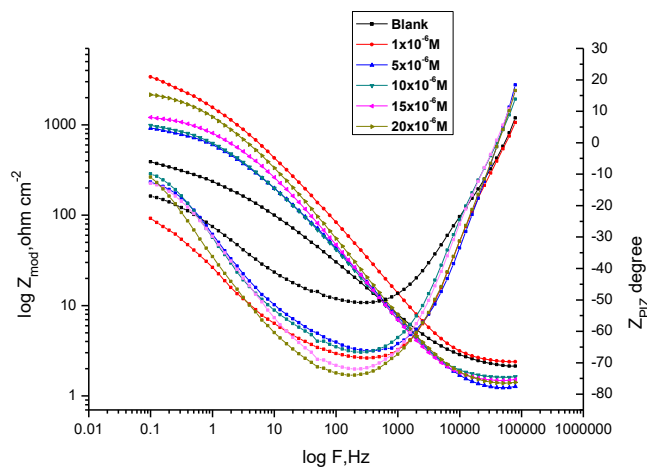


Figure 16. Bode plots recorded for brass in 1 M HNO₃ without and with various doses of PQD at 25°C

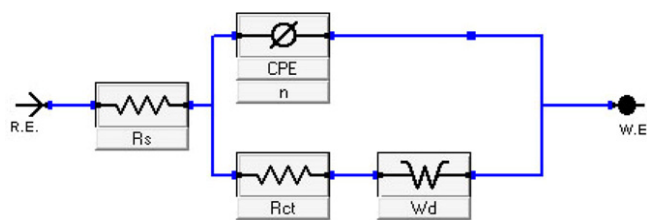


Figure 17. Electrical equivalent circuit used to fit the impedance data

Table 7. Electrochemical kinetic parameters obtained from EIS technique for Cu and α-brass in 1 M HNO₃ solution containing various doses of PQD at 25°C

Comp.	Conc.x10 ⁶ M	R _{ct} Ω cm ²	C _{dl} μFcm ⁻² 10 ⁻⁸	θ	%PE
Cu	Blank	115.6	270	--	--
	1	705.9	75	0.836	83.6
	5	1136	23	0.898	89.8
	10	1335	18	0.913	91.3
	15	2240	10	0.948	94.8
	20	3163	3.8	0.963	96.3
α-Brass	Blank	283.6	170	----	----
	1	690.8	110	0.588	58.8
	5	781.3	81	0.637	63.7
	10	877.4	72	0.676	67.6
	15	1567	25	0.819	81.9
	20	1739	6.7	0.836	83.6

The presence of PQD enhances the value of R_{ct} in acidic solution for Cu and α -brass. Values of C_{dl} are also brought down to the maximum extent in the presence of PQD and the decrease in the values of CPE follows the order similar to that obtained for i_{corr} in this study. The decrease in CPE/ C_{dl} results from a decrease in local dielectric constant and/or an increase in the thickness of the double layer, suggesting that the investigated PQD inhibits the Cu corrosion by adsorption at metal/acid [65].

3.4. EFM tests

EFM is a nondestructive corrosion measurement technique that can directly give values of the corrosion current without prior knowledge of Tafel constants. Like EIS, it is a small ac signal. Unlike EIS, however, two sine waves (at different frequencies) are applied to the cell simultaneously. Because current is a non-linear function of potential, the system responds in a nonlinear way to the potential excitation. The current response contains not only the input frequencies, but also contains frequency components which are the sum, difference, and multiples of the two input frequencies. The two frequencies may not be chosen at random. They must both be small, integer multiples of a base frequency that determines the length of the experiment. The great strength of the EFM is the causality factors which serve as an internal check on the validity of EFM measurement. The causality factors CF_2 and CF_3 are calculated from the frequency spectrum of the current responses. Figures(18a-g, 19a-g) show the frequency spectrum of the current response of pure Cu and brass in nitric acid solution, contains not only the input frequencies, but also contains frequency components which are the sum, difference, and multiples of the two input frequencies. The EFM intermodulation spectrums of Cu and brass in nitric acid solution containing (1×10^{-6} - 20×10^{-6} M) of PQD at 25°C are shown in Figures (18a-g, 19a-g). The harmonic and intermodulation peaks are clearly visible and are much larger than the background noise. The two large peaks, with amplitude of about $200 \mu\text{A}$, are the response to the 40 and 100 mHz (2 and 5 Hz) excitation frequencies. It is important to note that between the peaks there is nearly no current response ($<100 \text{ mA}$). The experimental EFM data were treated using two different models: complete diffusion control of the cathodic reaction and the "activation" model. For the latter, a set of three non-linear equations had been solved, assuming that the corrosion potential does not change due to the polarization of the working electrode. The larger peaks were used to calculate the corrosion current density (i_{corr}), the Tafel slopes (β_c and β_a) and the causality factors (CF_2 and CF_3). These electrochemical parameters were simultaneously determined by Gamry EFM140 software, and listed in Table 8 indicating that this extract inhibit the corrosion of Cu in 1 M HNO_3 through adsorption. The causality factors obtained under different experimental conditions are approximately equal to the theoretical values (2 and 3) indicating that the measured data are verified and of good quality [66]. The inhibition efficiencies IEEFM % increase by increasing the studied extract doses for either Cu or α -brass and was calculated as follows:

$$\% PE_{EFM} = \left(1 - \frac{i_{corr}}{i_{corr}^0}\right) \times 100 \quad (12)$$

Where i_{corr}^0 and i_{corr} are corrosion current densities in the nonexistence and existence of PQD respectively

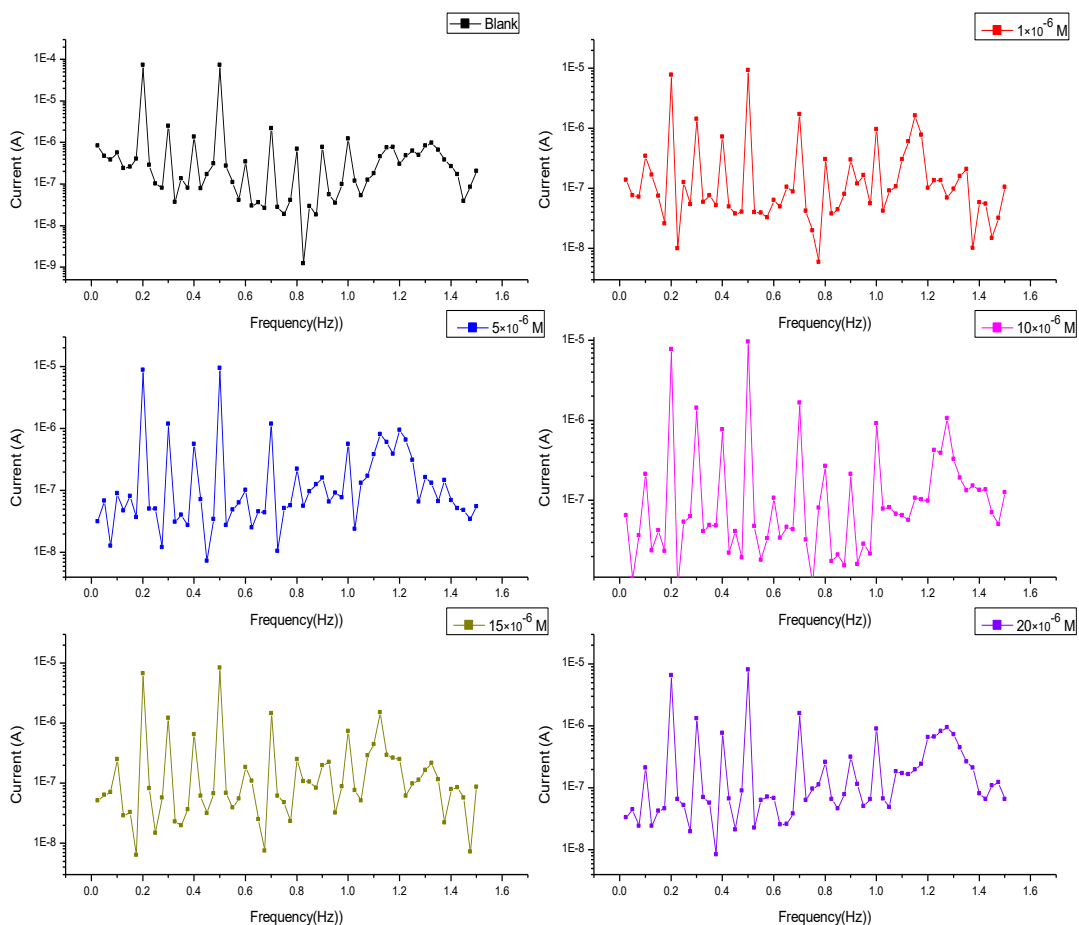


Figure 18(a-g). Intermodulation spectrums for the corrosion of Cu in 1 M HNO₃ without and with various doses of PQD at 25°C

Table 8. Electrochemical kinetic parameters obtained by EFM technique for Cu and α-brass in 1 M HNO₃ solution containing different doses of PQD at 25°C

Comp.	Conc, M	i_{corr} μAcm^{-2}	β_a $mVdec^{-1}$	β_c $mVdec^{-1}$	CF-2	CF-3	CR mpy	% PE
Cu	Blank	59.1	79.03	170.9	2.0	2.2	29.1	----
	1x 10 ⁻⁶	14.6	68.57	281.0	1.8	2.9	7.2	75.2
	5x 10 ⁻⁶	11.2	57.65	167.2	1.8	2.5	5.5	81.0
	10 x 10 ⁻⁶	9.49	50.90	85.47	2.0	3.0	4.6	83.9
	15x 10 ⁻⁶	9.02	56.65	148.0	1.9	2.3	4.4	84.7
	20x 10 ⁻⁶	6.97	44.91	99.24	1.7	2.9	3.4	88.2
α-Brass	Blank	49.0	116.8	151.5	1.9	2.3	68	----
	1x 10 ⁻⁶	22.9	65.56	89.9	1.8	2.9	11	53.1
	5 x 10 ⁻⁶	18.2	63.63	93.4	2.0	3.5	9	62.7
	10x 10 ⁻⁶	13.7	47.14	68.8	2.1	3.3	6	71.9
	15x 10 ⁻⁶	9.12	61.56	120	1.8	2.3	4	81.3
	20x 10 ⁻⁶	7.58	56.07	85.2	1.8	2.5	3	84.5

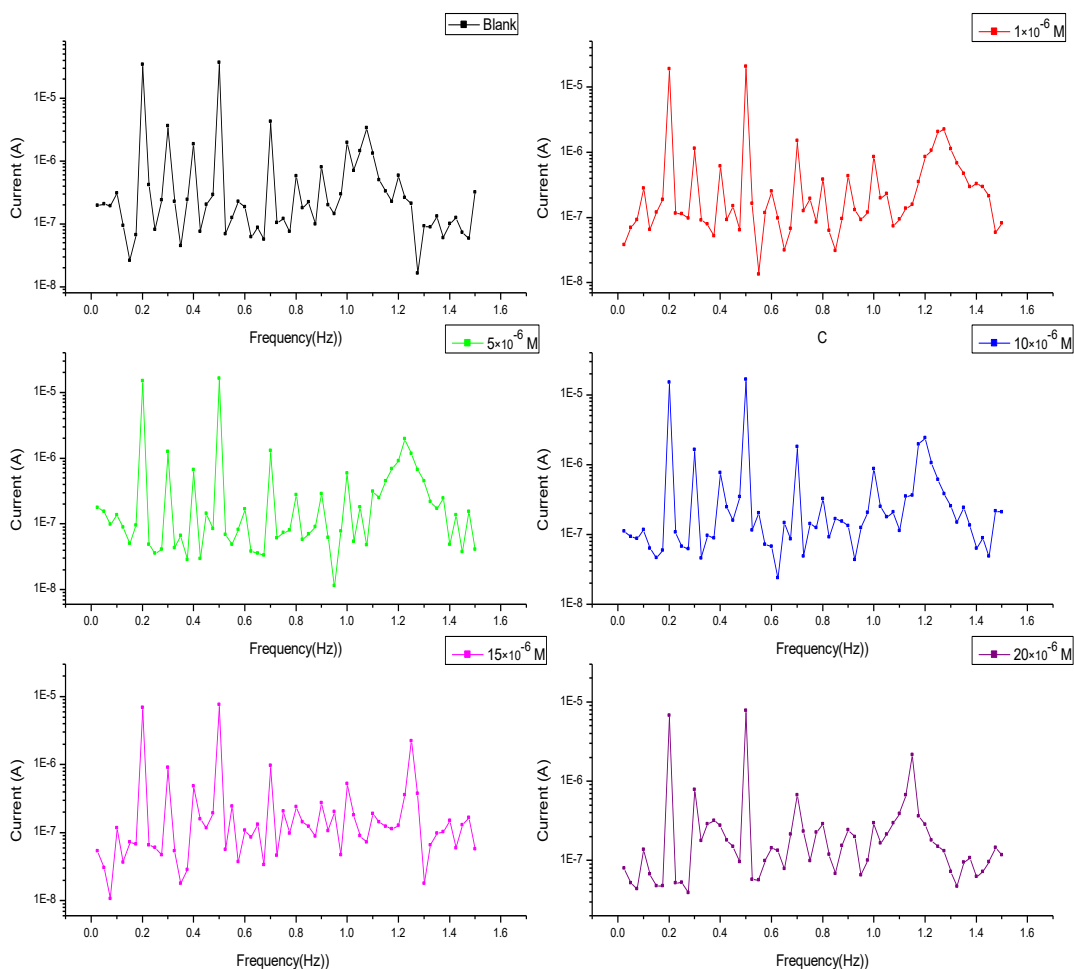


Figure 19(a-g). Intermodulation spectrums for the corrosion of α -brass in 1 M HNO₃ without and with various doses of PPD at 25°C

3.5. SEM/EDX analysis

In order to verify if the PPD in fact adsorbed on Cu and α -brass surface, both SEM and EDX experiments were carried out. The SEM micrographs for Cu and α -brass surface alone and after 24 h immersion in HNO₃ without and with the addition of 20x 10⁻⁶M of the tested PPD are shown in Figures (20a-c & 21a-c). As expected, Figures (20a, 21 a) shows metallic surface is clear, while in the absence of the PPD, the Cu and α -brass surface is damaged by HNO₃ corrosion (Figures (20b& 21b). In contrast, in the presence of the QD (Figures (20c & 21c)), the metallic surface seems to be almost no affected by corrosion. The corresponding EDX data are presented in Table 9. It is clear from the Table of Cu and α -brass in the presence of PPD, the existence of C and O which suggested the adsorption of the investigated PPD on the Cu and α -brass surface and confirm the formation of a thin film of PPD observed in SEM micrograph, thus protecting the surface against corrosion.

3.6. SEM analysis

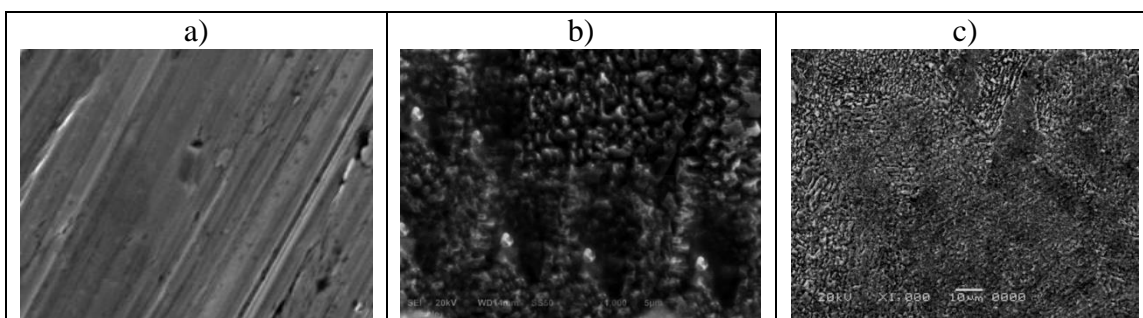


Figure 20. SEM micrographs of Cu surface (a) before of immersion in 1 M HNO₃, (b) after 24 h of immersion in 1 M HNO₃ and (c) after 24 h of immersion in 1 M HNO₃+ 20x 10⁻⁶ M of PQD at 25°C

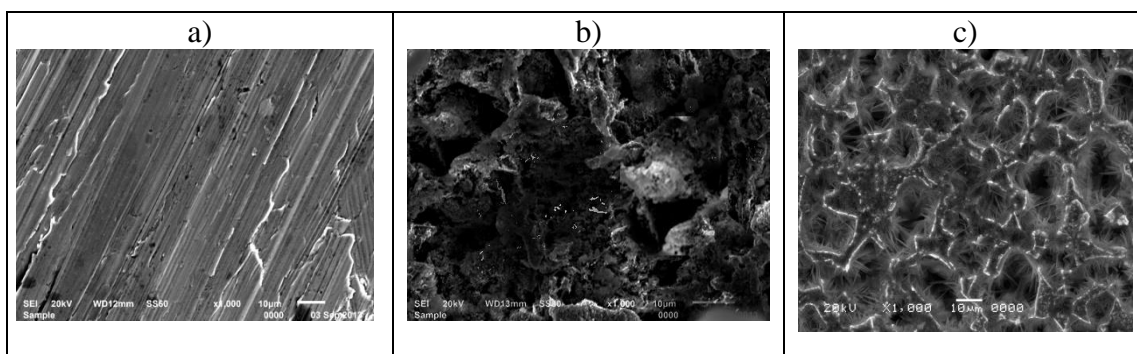


Figure 21. SEM micrographs of α -brass surface (a) before of immersion in 1 M HNO₃, (b) after 24 h of immersion in 1 M HNO₃ and (c) after 24 h of immersion in 1 M HNO₃+ 20x 10⁻⁶ M of PQD at 25°C

Table 9. Surface composition (weight %) of Cu and α brass before and after immersion in 1 M HNO₃ without and with 20x 10⁻⁶ M of PQD at 25°C

	(Mass %)	Cu	Zn	Si	Fe	O	N	C
Cu	Cu alone	97.7 7	--	--	--	0.4 3	--	--
	blank	79.1 3	--	--	--	5.8 5	--	14.1 1
	PQD	46.8 8	--	--	--	25. 36	14.9 7	12.5 4
α Brass	Brass alone	64.2 6	32.7 2	--	0.79	1.1 3	--	--
	blank	58.4 2	29.7 8	--	0.78	--	--	10.4 1
	PQD	35.1 5	20.2 1	0.21	--	15. 53	11.4 5	17.4 5

3.7. Mechanism of inhibition

From the observations drawn from the different methods, corrosion inhibition of Cu and brass in 1 M HNO₃ solution by PQD as indicated from weight loss, potentiodynamic polarization, EIS and EFM techniques were found to depend on the dose and the nature of the inhibitor [67].

PQD have active center for π -electron and lone pair of electron (presence of hetero atoms such as oxygen and nitrogen) and this causes the adsorption of the inhibitor on the surface on Cu is improved by their presence.

The adsorption of organic molecules on the solid surfaces cannot be considered only as purely physical or as purely chemical adsorption phenomenon. In addition to the chemical adsorption, inhibitor molecules can also be adsorbed on the Cu surface via electrostatic interaction between the charged metal surface and charged inhibitor molecule if it is possible [68]. The free energy of adsorption value is not very greater than -40 kJ mol^{-1} should indicate contribution of physical adsorption [51]. Consequently, from experimental findings, it is proposed that Cu corrosion can be inhibited with addition of PQD to 1 M HNO₃ solution by the following mechanism: PQD additive is physically adsorbed on cathodic sites of the Cu surface during the early stage of immersion time in HNO₃ solution, leading to retarded the dissolution Cu and α brass. The value of inhibition efficiency using this compound on Cu surface more than on α brass, due to α brass more active chemically and occur dezincification corrosion type. In addition to Cu need strong oxidizer such as nitric acid.

4. CONCLUSIONS

1. The organic compound namely PQD work as corrosion inhibitor to protect Cu metal brass in nitric acid solutions.
2. Using weight loss technique as the dose of PQD increases, the PE increases but decreases with an increase in temperature.
3. The inhibition of Cu and brass in 1 M HNO₃ solution was found to follows Langmuir adsorption isotherm.
4. The thermodynamic values obtained from this study indicate that the presence of PQD increases the activation energy and the negative values of ΔG_{ads}^0 indicate spontaneous adsorption of the inhibitors on the surface of Cu.
5. The results obtained from polarization potentiodynamic showed that the inhibiting properties increase with inhibitor dose.
6. Double layer capacitances decrease with respect to blank solution when PQD is added. This fact confirms the adsorption of PQD molecule on the Cu metal surface.
7. PQD adsorbed on Cu metal surface forming a barrier film and protect Cu substrate against corrosion in 1 M HNO₃ solution through the free electrons on the oxygen, nitrogen atoms in addition to a π electron interaction of the benzene nucleus.

8. From SEM and EDX analysis suggest the adsorption of PQD on the Cu and α -brass surface and confirm the formation of a thin film of Pyrimidoquinoline observed in SEM micrograph, thus protecting the surface against corrosion

8. The PE of the investigated compound determined by WL, PP, EFM and EIS techniques are in reasonably good agreement.

References

1. S. Kertit, H. Essoufi, B. Hammouti, M. Benkaddour, *Chim. Phys.* 95 (1998) 2070.
2. R. Karpagavalli, S. Rajeswari, *Anti-corr. Meth. and Mater.* 45 (1998) 333.
3. W.A. Badawy, F.M. Al-kharafi, *Corros. Sci.* 55 (1999) 268.
4. M.I. Abbas, *Br. Corros. J.* 26 (1991) 273.
5. S. Kertit, B. Hammouti, *Appl. Surf. Sci.* 93 (1996) 59.
6. S.S. El-Egamy, A.S. El-Azeb, W.A. Badawy, *Corros. Sci.* 50 (1994) 468.
7. S. El Issami, L. Bazzi, M. Mihit, M. Hilali, R. Salghi, E. AitAddi, *Physique IV* 123 (2003) 307.
8. Y. Abed, Z. Anaz, B. Hammouti, A. Aouinti, S. Kertit, A. Mansri, *J. Chim. Phys.* 96 (1999) 96.
9. S.N. Banerjee, *An introduction to science of corrosion and its inhibition*, Oxonian Press, New Delhi, 1985; p.286
10. K.F. Khaled, *Electrochim. Acta.* 54 (2009) 4345.
11. T. Kosec, D.K. Merl, I. Milošev, *Corros. Sci.* 50 (2008) 1987.
12. L.M. Rodriguez-Valdez, A. Martinez-Villafane, D. Glossman-Matnik, *J. Mol. Struct. THEOCHEM.* 713 (2005) 65.
13. E.M.Sherif, Su-Moon Park, *Electrochim. Acta* 51(2006) 6556
14. E.Szöcs, Gy.Vastag, A.Shaban, E.Kálmán, *Corros.Sci.*, 47 (2005) 893
15. R.Subramanian, V. Lakshminarayanan, *Corros. Sci.*, 44 (2002) 535
16. S. Ramesh, S.Rajeswari, *Corros.Sci.*, 47 (2005) 151
17. A.Lalitha, S. Ramesh, S. Rajeswari, *Electrochim. Acta* 51 (2005) 47
18. Da-quan Zhang, Li-xinGao, Guo-ding Zhou, *Corros. Sci.*, 46 (2004) 3031
19. J.L. Polo, P.Pinilla, E.Cano, J.M.Bastidas, *Corrosion*; 59(2003)414
20. L. Larabi, O.Benali, S.M.Mekelleche, Y.Harek, *Appl. Surf. Sci.*, 253 (2006)1371
21. E.M.Sherif, Su-Moon Park, *Electrochim. Acta* 51 (2006) 4665
22. E.M.Sherif, S.-M. Park, *J. Electrochem.Soc.* 152 (2005) B428
23. E.Stupnisek-Lisac, A.Brnada, A.D. Mance, *Corros. Sci.*, 42 (2000) 243
24. H. Ma, S. Chen, L. Niu, S. Zhao, S. Li, D. Li, *J. Appl. Electrochem.*32(2002)65
25. Maryam Ehteshamzadeh, TaghiShahrabi, MirghasemHosseini, *Anti-Corrosion Meth. Mater.* 53/5 (2006) 296
26. M.Ehteshamzade, T.Shahrabi, M.G.Hosseini, *Appl.Surf.Sci.* 252 (2006) 2949
27. A.A.ElWarraky, *Anti-corrosion meth. Mater.* 50(2003) 40
28. J.B. Matos, L.P.Pereira, S.M.L.Agostinho, O.E.Barcia, G.G.O.Cordeiro,E.D'Elia, *J. Electroanal. Chem.* 570 (2004) 91
29. G. Moretti, F. Guidi, *Corros.Sci.* 44 (2002) 1995 5
30. K. Barouni, L. Bazzi, R. Salghi, M. Mihit, B. Hammouti, A. Albourine, S. El Issami, *Mater.Lett.*62 (2008) 3325.
31. R.G. Parr, R.A. Donnelly, M. Levy, W.E. Palke, *J. Chem. Phys.* 68 (1978) 3801.
32. R.W. Bosch, J. Hubrecht, W.F. Bogaerts, B.C. Syrett, *Corrosion.* 57(2001) 60.
33. D.Q. Zhang, Q.R. Cai, X.M. He, L.X. Gao, G.S. Kim, *Mater. Chem. Phys.* 114 (2009) 612.
34. M.A. Ismail, S. Al-Shihry, R. K. Arafa, and U. El-Ayaan, *Journal of Enzyme Inhibition and Medicinal Chemistry*, 28 (2013) 530.

35. 35.A.K. Singh, M.A. Quraishi, *Corros. Sci.* 52 (2010)1378.
36. 36.K. K. Ai-Neami, A. K. Mohamed, I. M. Kenawy and A. S. Fouda, *Monatsh Chem.*, 126 (1995) 369.
37. K.F. Khaled, M.A. Amin, N.A. Al-Mobarak, *Appl. Electrochem.* 40 (2010) 601.
38. K.F. Khaled, S.A. Fadel-Allah, B. Hammouti, *Mater. Chem. Phys.* 117 (2009)148.
39. G.B. Ateya, B. El-Anadouli, F. El-Nizamy, *Corros. Sci.* 24 (1984) 509.
40. M. Kliskic, J. Radosevic, S. Gndic; *J. Appl. Electrochem.* 27 (1997) 947.
41. A. M. S. Abdel, A.El- Saied, *Trans. Soc. Adv. Electrochem. Sci. Technol.* 16 (1981)197.
42. A.J. Bard, L.R. Faulkner, *Electrochemical Method, John Wiley& Sons*, NY (1980).
43. F.M. Donahue, K. Nobe, *J. Electrochem. Soc.* 112 (1965) 886.
44. E. Kamis, F. Belluci, R.M. Latanision, E.S.H. El-Ashry, *Corrosion.* 47 (1991) 677.
45. T.P. Zhao, G.N. Mu, *Corros. Sci.* 41(1999) 1937.
46. A. Döner, G. Kardas, *Corros. Sci.* 53 (2011) 4223.
47. B.G. Ateya, B.E. El-Anadouli, F.M. El-Nizamy, *Corros. Sci.* 24 (1984) 509.
48. X.H. Li, S.D. Deng, H. Fu, G.N. Mu, *Corros. Sci.* 52 (2010) 1167.
49. G. Quartarone, G. Moretti, T. Bellomi, G. Capobianco, A. Zingales, *Corrosion.* 54 (1998) 606.
50. W.D. Bjorndahl, K. Nobe, *Corrosion.* 40 (1984) 82.
51. A. Schumacher, W. Muller, Stockel, J., *Electroanal. Chem.* 219 (1987) 311.
52. D.C. Silverman, J.E. Carrico, *Corrosion.* 44 (1988) 280.
53. W.J. Lorenz, F. Mansfeld, *Corros. Sci.* 21 (1981) 647.
54. D.D. Macdonald, M.C. Mckubre, Impedance measurements in Electrochemical systems, Modern Aspects of Electrochemistry, Vol. 14, Plenum Press, New York, 1982, p. 61
55. F. Mansfeld, *Corrosion*, 36 (1981) 301.
56. C. Gabrielli, Identification of Electrochemical processes by Frequency Response Analysis, Solarton Instrumentation Group, 1980.
57. M. El Achouri, S. Kertit, H.M. Gouttaya, B. Nciri, Y. Bensouda, L. Perez, M.R. Infante, K. Elkacemi, *Prog. Org. Coat.* 43 (2001) 267.
58. J.R. Macdonald, W.B. Johanson, Theory in Impedance Spectroscopy, John Wiley& Sons, New York, 1987.
59. S.F. Mertens, C. Xhoffer, B.C. Decooman, E. Temmerman, *Corrosion.* 53 (1997) 381.
60. Trabanelli, G., Montecelli, C., Grassi, V., Frignani, A., *J. Cem. Concr. Res.*, 35 (2005) 1804.
61. F.M. Reis, H.G. de Melo, I. Costa, *J. Electrochim. Acta.* 51(2006) 1780.
62. M. Lagrenee, B. Mernari, M. Bouanis, M. Traisnel, F. Bentiss, *Corros. Sci.* 44 (2002) 573.
63. E. McCafferty, N. Hackerman, *J. Electrochem. Soc.* 119 (1972) 146.
64. Y.M.Abdallah1 ,Hala M. Hassan, K.Shalabiand A.S. Fouda, *Int. J. Electrochem. Sci.*, 9 (2014)5073.
65. M.A. Hegazy, A. Abdel Nazeer, K. Shalabi ,*Journal of Molecular Liquids* 209 (2015) 419.
66. A.S. Fouda, K. Shalabi and A.A. Idress, *Green Chemistry Letters and Reviews*, 8 (3)(2015) 17.
67. A.S. Fouda,, K. Shalabi, A.A. Idress, *Int. J. Electrochem. Sci.*, 9 (2014) 5126.